Sensitivity of Spaceborne LiDAR, Optical, and SAR Features for Forest Biomass Modelling: A GEDI–Sentinel-2–SAOCOM Analysis

Eren Gursoy Ozdemir [1], Omer Gokberk Narin[2], Saygin Abdikan [3]

[1] Bartın University, Department of Architecture and Urban Planning, 74410 Bartın, Türkiye - eozdemir@bartin.edu.tr
[2] Afyonkocatepe University, Department of Geomatics Engineering, 03200 Afyonkarahisar,Türkiye -gokberknarin@aku.edu.tr
[3] Hacettepe University, Department of Geomatics Engineering, 06800 Ankara, Türkiye - sayginabdikan@hacettepe.edu.tr

Keywords: Biomass estimation, L-band, Lidar altimetry, GEDI, optical image

Abstract

This study evaluates the synergy of NASA’s Global Ecosystem Dynamics Investigation (GEDI) spaceborne LiDAR, Sentinel-2 multispectral imagery, and L-band Argentine Satellite System for Emergency Management (SAOCOM) 1A SAR data for aboveground biomass (AGB) estimation in the Belgrade Forest, Istanbul. Utilizing 1,356 GEDI L4A footprints as reference data, the research incorporates ten Sentinel-2 bands, five optical indices (NDVI, NDVIred, EVI, LSWI, CIre), SAR backscattering coefficients (σ°HH and σ°HV), polarimetric H/A/α polarimetric decomposition parameters and dual polarimetric radar vegetation indices, namely the Dual-Pol Radar Vegetation Index (DpRVI). High-dimensional feature spaces were optimized through ensemble-based, correlation-based, and hybrid RFECV selection strategies before evaluating four machine learning architectures: Multi-layer Perceptron (MLP), Kernel Ridge, Lasso, and Elastic Net. The MLP model achieved the highest predictive accuracy (R^2 = 0.20, RMSE = 62.93 Mg/ha, MAE = 51.31 Mg/ha), outperforming linear regularization models, which exhibited R^2 values between 0.15 and 0.16. Sensitivity analysis identified red-edge and SWIR bands, alongside indices such as NDVIred, LSWI, and CIre, as the most robust predictors, while the contribution of SAR-derived features remained comparatively limited. These findings underscore the efficacy of non-linear deep learning architectures and multi-source data fusion in resolving complex biophysical interactions within heterogeneous forest environments.

1. INTRODUCTION

Forests play a crucial role in carbon sequestration and in regulating interactions between the biosphere and the atmosphere. Accurate knowledge of forest biomass is essential for evaluating ecosystem sustainability and supporting efforts to mitigate climate change (Buotte et al., 2019). Conventional field-based approaches are labor-intensive, costly, logistically challenging, and generally limited to relatively small areas. Moreover, generating accurate biomass estimates at operational scales remains difficult, as the environmental, topographic, and biophysical heterogeneity of forest ecosystems across space and time constrains regional assessments of carbon sources and sinks (Lu, 2006).

The production of AGB data and maps generally utilizes terrestrial measurements based on biophysical properties and tree species-specific allometric equations (Sulabha et al., 2025). Recent advances in satellite remote sensing have greatly improved the ability to assess forest biomass and carbon stocks. Passive optical data, together with active sensors such as synthetic aperture radar (SAR) and light detection and ranging (LiDAR), provide robust means for characterizing forest ecosystem structure, composition, and aboveground biomass (AGB) (Lu et al., 2014). Optical imagery has long been employed for biomass estimation. It offers advantages such as high spatial resolution, spectral diversity, global monitoring, and frequent image acquisition. However, limited correlation with canopy closure may occur (Sulabha et al., 2025), and they also provide poor information about the vertical profile (Tian et al., 2023). Its utility also diminishes in dense forest environments due to spectral saturation.

In contrast, SAR systems penetrate vegetation and operate independently of atmospheric conditions, although their sensitivity to biomass is influenced by forest structural attributes (Ghasemi et al., 2013). Polarimetric SAR enables the separation of distinct scattering contributions within a single resolution cell, most commonly surface, volume, and double-bounce components, providing a valuable basis for isolating these mechanisms in forest applications (Tomar et al., 2019). One of the standout SAR features is the Dual-pole Radar Vegetation Index that provided good correlations with crop biophysical parameters (DpRVI) (Mandal et al., 2020). Yadav et al. (2022) also stated that L-band derived DpRVI showed better relationship with crop parameters compared to C-band data. Compared to the C-band, the L-band is preferred because its longer wavelength allows for better penetration. Studies conducted in tropical regions have shown that the vast majority of research is performed using only the L-band (Sulabha et al., 2025). The scattering mechanism can be derived through SAR decomposition of polarimetric data. The parameters of the H/A/α decomposition method have been applied to Sentinel-1 for vegetation analysis (Ghivarry et al., 2024).

Multi-sensor studies are also gaining prominence. SAR and optical data can provide a better estimation of AGB when used together. Ozdemir and Abdikan (2025) combined multi frequency SAR (SAOCOM, ALOS-2, Sentinel-1, TerraSAR-X) and Sentinel-2 data to estimate AGB of coniferous, deciduous, and mixed forest in Türkiye. They achieved a better result when SAOCOM, ALOS-2 and Sentinel-2 data were used together. Ghivarry et al. (2024) used Sentinel-1 data to estimate mangrove AGB provided by Global Ecosystem Dynamics Investigation (GEDI).

Spaceborne LiDAR offers a superior capability for resolving vertical vegetation structure, and the advent of NASA’s Global GEDI mission has enabled canopy height and biomass measurements at an unprecedented global scale (Sun et al., 2022).

https://doi.org/10.5194/isprs-archives-XLIX-B3-2026-1023-2026

A key application of GEDI observations is estimating aboveground forest biomass, with its 25 m footprint-level L4A products converted to Aboveground Biomass Density (AGBD) through calibration models developed from collocated field inventory and airborne laser scanning data (Dubayah et al., 2022a).

This study aims to estimate AGB in the northern İstanbul forests using L-band SAOCOM 1A SAR data by integrating backscatter and scattering-mechanism parameters, Sentinel-2 spectral bands, vegetation indices, and GEDI-derived biomass. The objectives are to assess the ability of these multi-source variables to capture biomass variability and to compare the performance of the proposed approach with existing AGB estimation methods. Feature selection methods are used to select contributing features when multiple features are generated. In this study, three methods (ensemble-based, correlation-based, and hybrid RFECV) were used, and prediction models were created using Multi-layer Perceptron (MLP), Kernel Ridge, Lasso, and Elastic Net machine learning algorithms. The study focused on three objectives: 1) Sensitivity analysis of features obtained from different sensors in biomass prediction, 2) Obtaining the most suitable model by comparing different methods, and 3) Comparing different feature selection methods.

2. DATA & METHOD

2.1. The Study Area

The study area is the Belgrade Forest, located in the European part of Istanbul, Türkiye (Figure 1). It exhibits transitional characteristics between Central European and Mediterranean climates. The region exhibits transitional climatic characteristics between Central European and Mediterranean climate regimes. Its vegetation structure primarily consists of deciduous tree and shrub species that shed their leaves during the winter months.

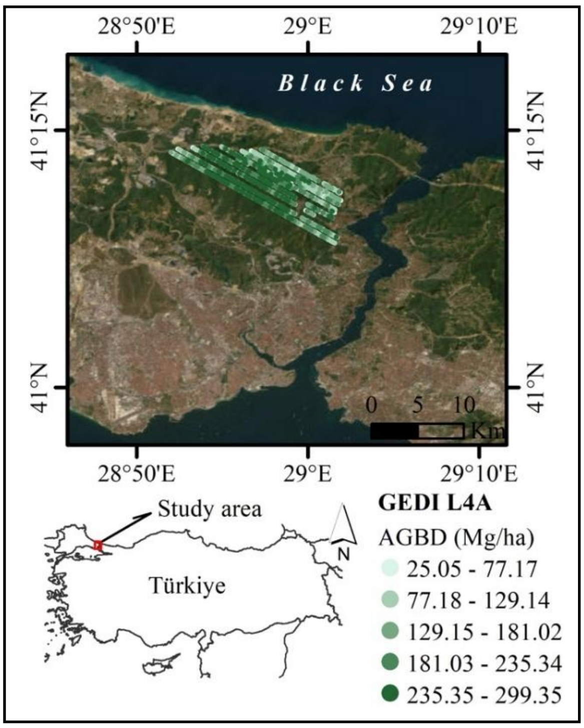

Figure 1. Map of the study area. Spatial distribution of the GEDI L4A dataset (n = 1,356).

2.2. Remote Sensing Data

Altimetry Data: GEDI
The study utilized three different remote sensing datasets. The GEDI L4A dataset provides AGBD data in units of Mg/ha. This AGBD data is derived from the relative height (RH) measurements in the GEDI Level 2A (L2A) dataset, which has ~25 m footprints (Dubayah et al., 2022b). The GEDI L4A data was downloaded using the Google Earth Engine (GEE) platform (Gorelick et al., 2017). The area was selected based on Belgrade Forest, and data from 2024 was downloaded. The GEDI L4A data was filtered, with the following criteria selected: l4_quality_flag =1, degrade_flag=0, and sensitivity > 0.95. Following the filtering stages, 1,234 GEDI L4A footprints were obtained on May 28, 2024, and 122 on October 21, 2024, for a total of 1,356. A total of 1,356 GEDI L4A footprints were used as the reference data for this study.

SAR Data: SAOCOM
Single date L-band SAOCOM imagery from May 2025 and was utilized to predict forest biomass. Pre-processing of the SAR data, which included radiometric calibration and terrain correction, as well as the extraction of polarimetric features, was performed using the European Space Agency's Sentinel Application Platform (SNAP 13.0) software. For predictive modeling, various features were derived from the SAOCOM data, incorporating backscattering coefficients (σ°HH and σ°HV). Entropy, Anisotropy, and Alpha Angle of polarimetric parameters derived from H/A/α decomposition, and specific dual-polarimetric radar vegetation indices, namely the Dual-Pol Radar Vegetation Index (DpRVI) is also obtained.

Optical Data: Sentinel-2
The study utilized Sentinel-2 data as the optical dataset. Sentinel-2 is a multispectral satellite dataset with a spatial resolution of 10 m, developed for the monitoring of land surfaces, vegetation analysis, and the determination of land use (Drusch et al., 2012). Atmospheric and geometric corrections were applied to the Sentinel-2 L2A images (COPERNICUS/S2_SR_HARMONIZED), which were downloaded using the GEE platform. A composite image was created by calculating the median of the pixel values from the cloud-free Sentinel-2A/B images from May 2024. The study utilized 10 Sentinel-2 bands (B2, B3, B4, B5, B6, B7, B8, B8A, B11, B12) and 5 indices (Normalized Difference Vegetation Index (NDVI), NDVIred, Enhanced Vegetation Index (EVI), Land Surface Water Index (LSWI), Chlorophyll Index - Red-Edge (CIre)) (Table 1).

Platform	Index	Equation	References
Sentinel-2	NDVI	$\frac{(\mathrm{NIR} - \mathrm{Red})}{(\mathrm{NIR} + \mathrm{Red})}$	Rouse et al., 1974
	NDVIred	$\frac{(\mathrm{NIR} - Red_{edge})}{(\mathrm{NIR} + Red_{edge})}$	Barnes et al., 2000
	LSWI	$\frac{(\mathrm{NIR} - \mathrm{SWIR})}{(\mathrm{NIR} + \mathrm{SWIR})}$	Xiao et al., 2004
	CIre	$\left(\frac{\mathrm{NIR}}{Red_{edge}}\right) - 1$	Gitelson and Merzlyak, 1994
	EVI	$\frac{2.5(\mathrm{NIR} - \mathrm{Red})}{(\mathrm{NIR} + 6\mathrm{Red} - 7.5\mathrm{Blue} + 1)}$	Huete et al., 1997

Table 1. List of optical indices used for AGBD estimation

The workflow for the study is shown in Figure 2. After obtaining satellite data for the region, preprocessing steps were completed. Then, various features were created from SAR and optical data, and a total of 27 variables were considered. Feature selection and optimization steps were performed for these variables, and machine learning methods were applied. Accuracy values were generated through validation and assessment steps.

2.3. Feature Selection and Optimization

To optimize the high-dimensional feature space and ensure model robustness, three distinct feature selection strategies ensemble-based, correlation-based, and hybrid Recursive Feature Elimination with Cross-Validation (RFECV) were implemented. The hybrid RFECV approach was specifically designed to integrate the importance-ranking capabilities of statistical estimators with the iterative refinement of recursive wrapper methods. This "hybrid" structure aims to mitigate multicollinearity by evaluating feature importance within a cross-validation framework, thereby isolating a non-redundant subset of predictors tailored for biomass estimation. Concurrently, the ensemble-based strategy was used to leverage tree-based importance measures, providing a descriptive mechanism for identifying biophysical linkages across the heterogeneous forest structure.

2.4. Regression Models

Following the feature optimization phase, four machine learning (ML) architectures; Multi-layer Perceptron (MLP), Kernel Ridge, Lasso, and Elastic Net were implemented to estimate AGB. The MLP model was configured with a 100–50 hidden-unit architecture, a hierarchical design intended to extract multi-level abstractions from the diverse spectral and radar inputs.
Kernel Ridge Regression combines classical Ridge Regression (L2-regulated linear regression) with kernel methods. It allows modeling nonlinear relationships (Murphy, 2012).
Least Absolute Shrinkage and Selection Operator (Lasso) is a sort of linear regression which uses a regularization technique to prevent overfitting and perform feature selection (Tibshirani, 1996). Elastic Net combines two different regularization approaches (L1 Lasso and L2 Ridge) to overcome fitting problems (Hans, 2011).

2.5. Accuracy Metrics & Methodology

To ensure statistical reliability and assess the generalizability of the models, The GEDI data were separated into 70% for training and 30% for testing. A k-fold cross-validation with a 5 repetition was applied for the reliability of the model. The predicted values were compared with the coefficient of determination (R^2) (Equation 1), Root Mean Squared Error (RMSE) (Equation 2), and Mean Absolute Error (MAE) (Equation 3).

$$R^2 = 1 - \frac{\sum_{i=1}^{n}(y_i - \hat{y}_i)^2}{\sum_{i=1}^{n}(y_i - \bar{y})^2} \tag{1}$$

$$\text{RMSE} = \sqrt{\frac{1}{n}\sum_{i=1}^{n}(y_i - \hat{y}_i)^2} \tag{2}$$

$$\text{MAE} = \frac{1}{n}\sum_{i=1}^{n}|y_i - \hat{y}_i| \tag{3}$$

where y_i is the GEDI L4A AGBD values, $\hat{y}_i$ is the estimated AGBD values, $\bar{y}$ is the mean of the GEDI L4A AGBD values.

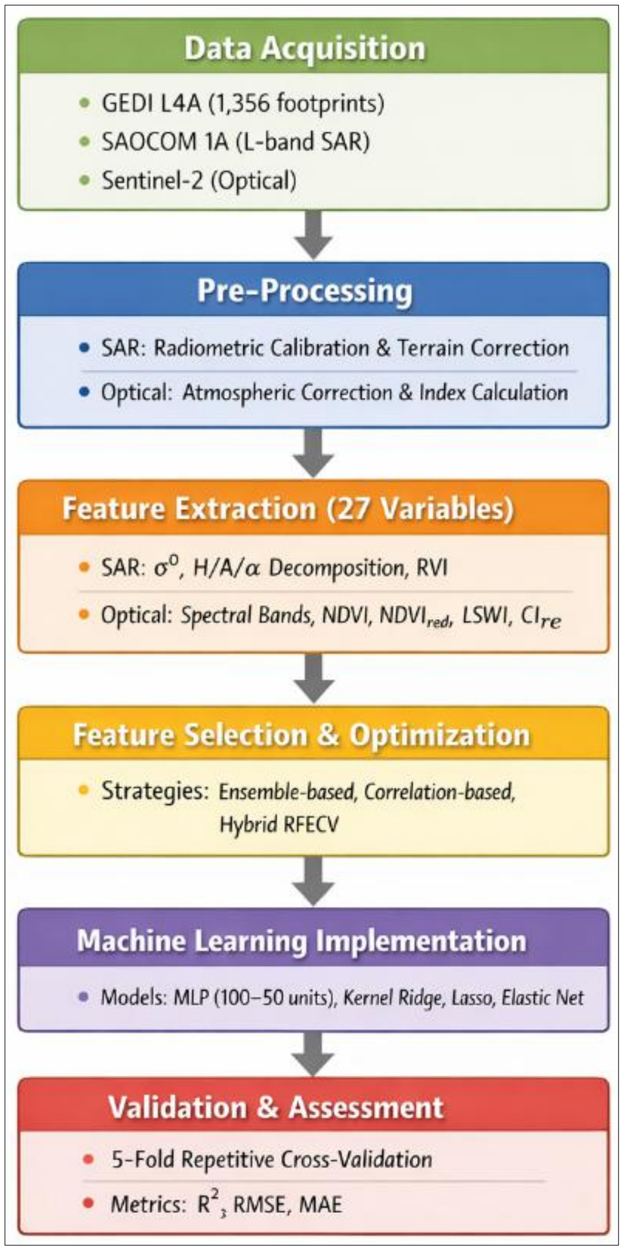

Figure 2. Workflow diagram showing the synergy of spaceborne LiDAR, polarimetric SAR, and optical data fusion for forest biomass modelling

3. RESULTS & DISCUSSION

The predictive performance of the evaluated machine learning models revealed a distinct advantage for non-linear architectures in capturing the complex biophysical relationships of the Belgrade Forest. Among the implemented algorithms, the MLP achieved the highest predictive accuracy with R^2 of 0.20, followed closely by Kernel Ridge Regression (R^2 = 0.19). In contrast, linear regularization-based models, such as Lasso (R^2 = 0.16) and Elastic Net (R^2 = 0.15), exhibited comparatively lower performance. As illustrated in Figure 3, these results indicate the limited capacity of linear frameworks to resolve the highly non-linear structure of biomass–spectral relationships in heterogeneous forest environments.

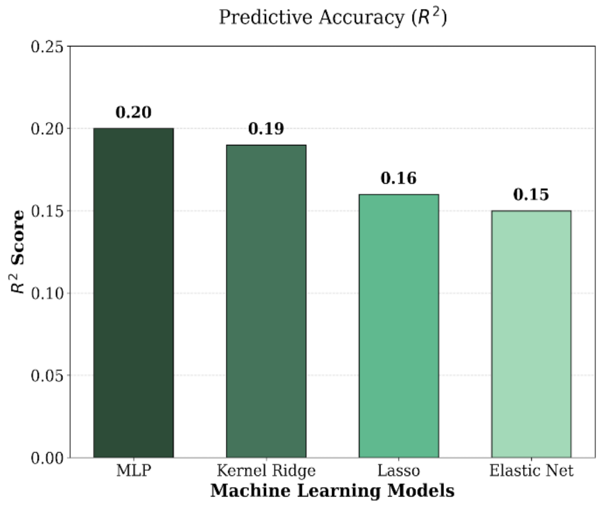

Figure 3. Comparison of Predictive Accuracy (R^2) among the evaluated ML models for AGB estimation

The evaluation of error metrics further reinforced the predictive superiority of the non-linear modeling approaches. Specifically, the MLP model achieved the lowest estimation uncertainty, yielding an RMSE of 62.93 Mg/ha and an MAE of 51.31 Mg/ha. This reduction in error relative to linear baselines highlights the efficacy of deep learning architectures in mitigating the residuals that often arise from the biophysical complexity of heterogeneous forest structures. As illustrated in Figure 4, the Kernel Ridge regression followed closely with an RMSE of 63.50 Mg/ha. However, the performance gap widened with the linear regularization models; the Elastic Net yielded the highest deviation (RMSE = 65.08 Mg/ha, MAE = 53.54 Mg/ha). These findings suggest that while linear models provide a computationally efficient baseline, they lack the sensitivity required to resolve subtle backscatter and spectral variations associated with varying biomass densities.

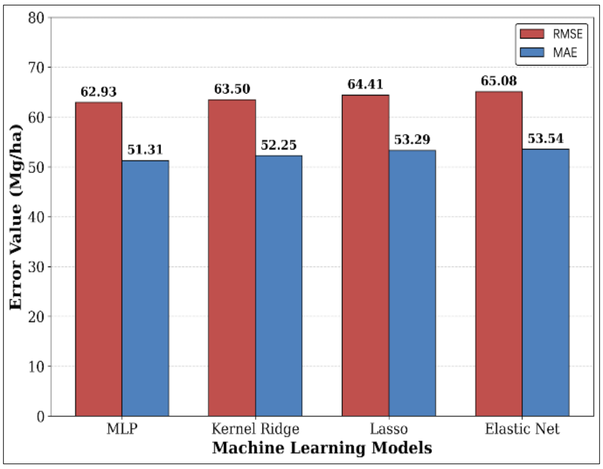

Figure 4. Comparison of Error Metrics (RMSE and MAE) across the four ML models

A second-level analysis incorporating various data transformations and three distinct feature selection strategies provided deeper insights into model stability and feature relevance. Feature selection results indicated that red-edge bands (B5, B6), shortwave infrared bands (B11, B12), and vegetation indices sensitive to canopy moisture and chlorophyll (NDVIred, LSWI, CIre) were consistently selected among top-performing feature subsets. This consistency reflects their strong biophysical linkage to canopy biomass in the study area. Notably, the ensemble-based feature selection produced the most stable subsets across the models, underscoring the effectiveness of tree-based importance measures in high-dimensional remote sensing data (see Figure 5).

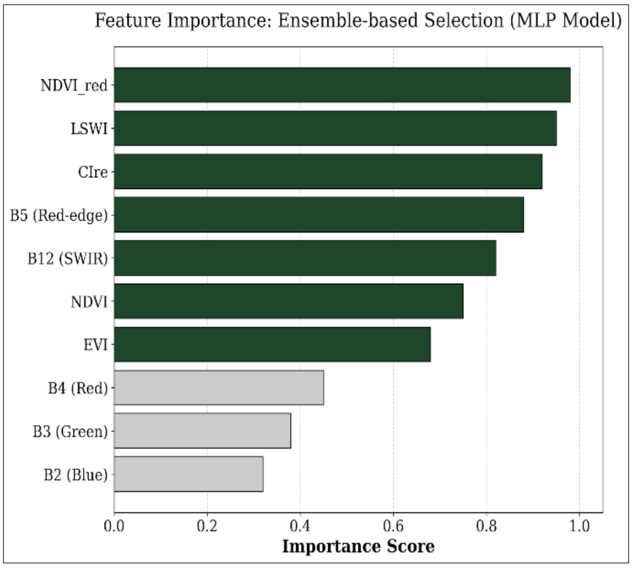

Figure 5. Feature Importance Scores of the top-performing features identified through the ensemble-based selection method for the MLP model

A comprehensive overview of these performance metrics and the optimized feature subsets is summarized in Table 2. The synthesis of these results highlights the superiority of the MLP model, which effectively leveraged the ensemble-based feature selection to identify the most robust predictors. While the linear models incorporated SAR features such as SAOCOM HH (dB) and Anisotropy, they did not match the accuracy of the MLP and Kernel Ridge architectures. This confirms that the MLP's hierarchical learning capability, when paired with strategic spectral indices, provides a more resilient framework for capturing complex biomass interactions than linear models relying on individual SAR backscatter parameters.

Ghivarry et al. (2024) achieved an R-squared of 0.2 using backscatter and decomposition of Sentinel-1 data over a mangrove forest to predict biomass from GEDI data. Model performance did not improve with dual-polarimetric data. Zurqani (2025) analysed GEDI data with Sentinel-1 and Sentinel-2 using different ML (Random Forest (RF), Classification and Regression Trees (CART), Gradient Tree Boosting (GTB), and Support Vector Machine (SVM)) methods. The study found that the GTB method provided the highest performance with the combination of Sentinel-2 and topography. In our case, our R^2 values vary between 0.15 and 0.20. The best R-square is around 0.2, similar to Ghivarry et al. (2024); however, in our case, Sentinel-2 provides the contribution, which is also shown by Zurqani (2025).

No	Model	R^2	RMSE	MAE	Feature Selection Methods	Feature List
1	MLP	0,20	62,93	51,31	Ensemble-based	B2, B3, B4, B5, B12, NDVI, NDVIred, CIre, LSWI, EVI
2	Kernel Ridge	0,19	63,50	52,25	Correlation-based	B2, B3, B4, B5, B12, NDVI, NDVIred, CIre, LSWI, EVI
3	Lasso	0,16	64,41	53,29	Correlation-based	Saocom_Anisotropy, Saocom_HH (dB), B2, B3, B4, B5, B6, B7, B8, B11, B12, NDVI, EVI
4	Elastic Net	0,15	65,08	53,54	Hybrid RFECV	B2, B3, B4, B5, B6, B7, B8, B8A, Saocom_HH(dB), NDVI, CIre

Table 2. Results of the model predictions

Mohite et al., (2024) estimated national biomass of India through GEDI and multi-source Earth observation data. In addition to Sentinel-1 and 2 variables, topography, soil, and forest attributes were also used in the estimation. Analyses were performed with different variables in different scenarios. The R^2 values obtained with only Sentinel-1 and 2 variables ranged between 0.55 and 0.6. However, it was observed that the R^2 values increased with the addition of other data. In our study, only L-band SAOCOM, Sentinel-2, and variables derived from these data were used. The results can be increased by using ancillary data.

4. CONCLUSIONS AND FUTURE PERSPECTIVES

Determining the AGB plays an important role in studies of the carbon cycle and climate change in the global ecosystem. In the combat against climate change, monitoring and estimating forest biomass at regional and global levels is of critical importance. Considering that obtaining AGB through terrestrial methods is costly and time-consuming, remote sensing systems and methods can provide an alternative for terrestrial studies.

In this study, GEDI data were used for model training and validation of the models, and L-band SAR and optical data were used to predict the GEDI data. The best results were achieved by an ensemble-based feature selection method with Sentinel-2 data and the spectral indices generated from these data. Although SAR data provided better results than some models, its contribution was limited. In the MLP method, which yields the best results, it is observed that the top three features obtained using ensemble-based methods are spectral indices generated from optical data, and NIR and Red-edge bands stand out as common bands.

The limitation of the study is that it was conducted in only one area. The methodology is also planned to be applied in regions with different forest species. As suggested in the previous studies, the next phase of the study plans to use topography and multitemporal data in combination with Sentinel-1 data. Additionally, NISAR data, which provides another L-band image, can also be used in this context. Different ML methods will also be tried.

Acknowledgments
The authors would like to thank the National Commission for Space Activities of Argentina (CONAE) for SAOCOM data. This study was supported by the Scientific and Technological Research Council of Türkiye (TÜBİTAK) under grant number 2224-A.

REFERENCES

Barnes, E.M., Clarke, T.R., Richards, S.E., Colaizzi, P.D., Haberland, J., Kostrzewski, M., Waller, P., Choi, C., Riley, E., Thompson, T., Lascano, R.J., Li, H., Moran, M.S., 2000. Coincident detection of crop water stress, nitrogen status and canopy density using ground-based multispectral data. In: Proc. 5th International Conference on Precision Agriculture, 1–15.

Buotte, P., Law, B., Ripple, W., Berner, L., 2019. Carbon sequestration and biodiversity co-benefits of preserving forests in the western United States. *Ecological Applications*, 30, e02039.

Drusch, M., Del Bello, U., Carlier, S., Colin, O., Fernandez, V., Gascon, F., et al., 2012. Sentinel-2: ESA's optical high-resolution mission for GMES operational services. *Remote Sensing of Environment,* 120, pp. 25–36.

Dubayah, R., Armston, J., Healey, S.P., Bruening, J.M., Patterson, P.L., Kellner, J.R., Duncanson, L., Saarela, S., Ståhl, G., Yang, Z., Tang, H., Blair, J.B., Fatoyinbo, L., Goetz, S., Hancock, S., Hansen, M., Hofton, M., Hurtt, G., Luthcke, S., 2022a. GEDI launches a new era of biomass inference from space. *Environmental Research Letters*, 17, 095001.

Dubayah, R.O., J. Armston, J.R. Kellner, L. Duncanson, S.P. Healey, P.L. Patterson, S. Hancock, H. Tang, J.M. Bruening, M.A. Hofton, J.B. Blair, S.B. Luthcke. 2022b. GEDI L4A Footprint Level Aboveground Biomass Density, Version 2.1. ORNL DAAC, Oak Ridge, Tennessee, USA. https://doi.org/10.3334/ORNLDAAC/2056

Ghasemi, N., Sahebi, M.R., Mohammadzadeh, A., 2013. Biomass estimation of a temperate deciduous forest using wavelet analysis. *IEEE Transactions on Geoscience and Remote Sensing*, 51, 765–776.

Ghivarry, G., Kutchartt, E., Pirotti, F., 2024: Assessing the potential of polarimetric decomposition of Sentinel-1 SAR for the estimation of mangrove forest biomass, Int. Arch. Photogramm. Remote Sens. Spatial Inf. Sci., XLVIII-3-2024, 183–190.

Gitelson, A.A., Merzlyak, M.N., 1994. Quantitative estimation of chlorophyll using reflectance spectra. *Journal of Photochemistry and Photobiology* B 22, 247–252.

Gorelick, N., Hancher, M., Dixon, M., Ilyushchenko, S., Thau, D., Moore, R., 2017. Google Earth Engine: Planetary-scale geospatial analysis for everyone. *Remote sensing of Environment*, *202*, 18-27.

Hans, C. 2011. Elastic net regression modeling with the orthant normal prior. *J. Am. Stat. Assoc. 106*, 1383–1393.

Huete, A.R., Liu, H.Q., Batchily, K., van Leeuwen, W., 1997. A comparison of vegetation indices over a global set of TM images for EOS-MODIS. *Remote Sensing of Environment*, 59, 440–451.

Lu, D., 2006. The potential and challenge of remote sensing-based biomass estimation. *International Journal of Remote Sensing*, 27(7), 1297–1328.

Lu, D., Chen, Q., Wang, G., Liu, L., Li, G., Moran, E., 2014. A survey of remote sensing-based aboveground biomass estimation methods in forest ecosystems. *International Journal of Digital Earth*, 9(1), 63–105.

Mandal, D., Kumar, V., Ratha, D., Dey, S., Bhattacharya, A., Lopez-Sanchez, J.M., McNairn, H., Rao, Y.S., 2020. Dual polarimetric radar vegetation index for crop growth monitoring using Sentinel-1 SAR data. *Remote Sensing of Environment*, 247, 111954.

Mohite, J., Sawant, S., Pandit, A., Sakkan, M., Pappula, S., Parmar, A., 2024. Forest aboveground biomass estimation by GEDI and multi-source EO data fusion over Indian forest, *International Journal of Remote Sensing*, 45:4, 1304-1338.

Murphy, K. P. 2012. Machine Learning: A Probabilistic Perspective - chapter 14.4.3, pp. 492-493, The MIT Press,

Ozdemir, EG, Abdikan, S., 2025. Forest Aboveground Biomass Estimation in Küre Mountains National Park Using Multifrequency SAR and Multispectral Optical Data with Machine-Learning Regression Models. *Remote Sensing*.; 17(6):1063

Rouse, J.W., Haas, R.H., Scheel, J.A., Deering, D.W., 1974. Monitoring vegetation systems in the Great Plains with ERTS. In: Proceedings of the Third Earth Resources Technology Satellite (ERTS) Symposium, NASA SP-351, pp. 48–62.

Sulabha, A.A., Asok, S.V., Reddy, C.S. *et al.* 2025. Aboveground Biomass Estimation in Tropical Forests: Insights from SAR Data—A Systematic Review. *J Indian Soc Remote Sens* 53, 653–679.

Sun, M., Cui, L., Park, J., García, M., Zhou, Y., Silva, C.A., He, L., Zhang, H., Zhao, K., 2022. Evaluation of NASA's GEDI lidar observations for estimating biomass in temperate and tropical forests. *Forests*, 13, 1686.

Tian, L, Wu, X, Tao, Y, Li, M, Qian, C, Liao, L, Fu, W. Review of Remote Sensing-Based Methods for Forest Aboveground Biomass Estimation: Progress, Challenges, and Prospects. *Forests*. 2023; 14(6):1086.

Tibshirani, R., 1996. Regression shrinkage and selection via the lasso. Journal of the Royal Statistical Society: Series B (Methodological), 58(1), pp. 267–288.

Tomar, K.S., Kumar, S., Tolpekin, V.A., 2019. Evaluation of hybrid polarimetric decomposition techniques for forest biomass estimation. *IEEE Journal of Selected Topics in Applied Earth Observations and Remote Sensing*, 12(10), 3712–3718.

Xiao, X., Hollinger, D., Aber, J.D., Goltz, M., Davidson, E.A., Zhang, Q.Y., 2004. Satellite-based modeling of gross primary production in an evergreen needleleaf forest. *Remote Sensing of Environment*, 89, 519-534

Yadav, V. P., Prasad, R., Bala, R., Srivastava, P. K., Vanama, V. S. K., 2022. Appraisal of dual polarimetric radar vegetation index in first order microwave scattering algorithm using sentinel – 1A (C - band) and ALOS - 2 (L - band) SAR data. *Geocarto International*, *37*(21), 6232–6250.

Zurqani, H.A. 2025. A multi-source approach combining GEDI LiDAR, satellite data, and machine learning algorithms for estimating forest aboveground biomass on Google Earth Engine platform, *Ecological Informatics* 86, 103052.